Journal of Catalysis 263 (2009) 146–154

Contents lists available at ScienceDirect

Journal of Catalysis

www.elsevier.com/locate/jcat

Catalysts based on platinum–tin and platinum–gallium in close contact for the selective hydrogenation of cinnamaldehyde

A.J. Plomp [a], D.M.P. van Asten [a], A.M.J. van der Eerden [a], P. Mäki-Arvela [b], D.Yu. Murzin [b], K.P. de Jong [a], J.H. Bitter [a,*]

[a] Inorganic Chemistry and Catalysis, Utrecht University, PO Box 80083, 3508 TB Utrecht, The Netherlands
[b] Laboratory of Industrial Chemistry and Reaction Engineering, Åbo Akademi, Biskopsgatan 8, FI-20500 Turku, Finland

ARTICLE INFO

Article history:
Received 12 December 2008
Revised 4 February 2009
Accepted 4 February 2009
Available online 27 February 2009

Keywords:
Selective hydrogenation
Platinum
Carbon nanofibers
Reductive deposition precipitation
Surface redox reaction
EXAFS

ABSTRACT

Bimetallic platinum–tin and platinum–gallium catalysts supported on carbon nanofibers (CNF) were prepared via reductive deposition precipitation and impregnation. Detailed EXAFS, TEM-EDX and XPS studies showed that reductive deposition precipitation resulted in a close contact of tin with platinum. These bimetallic catalysts displayed an improved selectivity for cinnamaldehyde hydrogenation towards the desired cinnamyl alcohol as compared to the monometallic platinum catalyst and a bimetallic catalyst prepared by impregnation in which such a close interaction was absent. The general applicability of reductive deposition precipitation as synthesis technique was demonstrated using tin and gallium as promoters.

1. Introduction

Platinum supported on carbon nanofibers (CNF) turned out as one of the most active catalysts for the hydrogenation of cinnamaldehyde [1,2]. To achieve this high activity, it was crucial to remove the majority of the oxygen surface groups from the CNF catalysts. These oxygen surface groups were initially indispensible for obtaining a high platinum dispersion [1,3]. In general the activity for hydrogenation was high, while the selectivity towards the desired cinnamyl alcohol was low [1,2,4]. Therefore the challenge is to increase the selectivity of these Pt/CNF catalysts while maintaining a high activity. Addition of a promoter metal(oxide) to CNF supported platinum catalysts is a promising route, since successful promotion of platinum based catalysts by tin, germanium, gallium or iron has been reported [5–10].

In early studies, the promoter salts were added in the reactor during the hydrogenation [7–9]. Though successful in enhancing the selectivity, it is not a very practical method for application in a continuous process. It is more convenient to make the promoter part of the catalyst. Various ways to prepare bimetallic catalysts for different applications have been reported [10]. The majority of these bimetallic catalysts are prepared using impregnation techniques. Unfortunately, this technique does not necessarily result in a close contact of the two metals, which is assumed to be of importance. Moreover, identification of the nature of the bimetallic phase remains challenging [10]. Controlled surface reactions of organometallic compounds have also been reported [10]. In that method one of the organic ligand moieties of the promoter–complex reacts with adsorbed hydrogen on the metal surface to bind the organometallic compound to the metal surface. Major drawback of this route is the risk of deposition of the organometallic complex on the support surface which results in multiple (inactive) phases on the catalyst [10].

Another promising technique to prepare bimetallic catalysts is the deposition of the second metal(oxide) via redox chemistry catalyzed by the first metal [11]. This technique is here referred to as reductive deposition precipitation (RDP). Barbier and coworkers [12,13] were among the first to use this technique to prepare bimetallic catalysts. In this case hydrogen was adsorbed on a metal based catalyst and the promoter was deposited via reduction of promoter-salt by the adsorbed hydrogen. Platinum–tin and platinum–iron catalysts have been prepared successfully in that way [13–16]. In a review of Mallat et al. [17] deposition of lead, bismuth or copper on palladium catalysts using RDP has also been described. Preparation of bimetallic catalysts via RDP can also be performed below the equilibrium potential of the redox reaction. The latter situation results in underpotential deposition: adatoms can be deposited on particular sites of the metal surface whereby the equilibrium potential is shifted and enables creation of submonolayers of adatoms [12,17].

Though the advantage of RDP for catalytic performance has been demonstrated [13,14], detailed characterization of the interaction of promoters with the active metal is lacking thus far. There-

* Corresponding author.
E-mail address: j.h.bitter@uu.nl (J.H. Bitter).

0021-9517/$ – see front matter
doi:10.1016/j.jcat.2009.02.003

Table 1
Synthesis details of RDP-prepared catalysts.

Precursor	Solvent	Intended Pt/promoter molar ratio
$SnCl_4$ (Sigma–Aldrich)	Aqueous HCl-solution, pH 1	5, 3, 1
$Sn(HCOO)_2$ (prepared from SnC_2O_4 (Fluka))	60 wt% formic acid at pH 3.9 (via addition of ammonium hydroxide)	5
$Ga(NO_3)_3{\cdot}xH_2O$ (Acros)	Demineralized water	5

fore, in this study we investigated the platinum–promoter interaction for RDP-prepared, CNF-supported bimetallic catalysts using TEM-EDX, XPS and EXAFS. These results will be related to catalytic results using the selective hydrogenation of cinnamaldehyde as a showcase [5,18]. Bimetallic Pt/CNF catalysts were prepared by deposition of tin(IV), tin(II) and gallium(III) compounds on the monometallic Pt/CNF catalyst via RDP. Tin(II) and gallium(III) combinations with platinum were prepared and characterized to investigate the role of underpotential deposition on the selective hydrogenation of cinnamaldehyde. To the best of our knowledge, deposition of gallium in this way has not been reported before. For comparison, a catalyst without a close platinum–promoter interaction prepared via impregnation of tin(IV)chloride on Pt/CNF has been included in the study.

2. Experimental

A Ni/SiO_2 (20 wt% nickel) growth catalyst was prepared via homogeneous deposition precipitation (HDP) using 17.0 g silica (Degussa, Aerosil 200), 21.1 g nickel nitrate hexahydrate (Acros; 99%) and 13.9 g urea (Acros; p.a.) in 1 L demineralized water according to an earlier described procedure [19].

CNF were grown from $CO/H_2/N_2$ at 823 K using Ni/SiO_2 (2 g) as reported earlier [4]. The raw CNF material (30 g) was collected and refluxed three times for 1 h per reflux in an aqueous KOH solution (1 M; 0.6 L; Merck; p.a.) to remove the SiO_2. After washing, the material was refluxed two times for 1 h per reflux in concentrated nitric acid (0.6 L; Merck; 65%) to remove exposed nickel and introduce oxygen surface groups on the CNF surface. After subsequent washing for three times with demineralized water and drying overnight at 393 K, the sample was denoted as CNF-ox.

Platinum was deposited via HDP on CNF-ox using $Pt(NH_3)_4(NO_3)_2$ and urea as base as described earlier [1]. The catalyst was reduced at 473 K for 1 h (heating rate 5 K/min) in a H_2/N_2 flow (100 mL/min; 10% v/v). The obtained material was denoted as Pt/CNF. Part of this monometallic catalyst was treated at 973 K for 2 h, to remove the oxygen surface groups, in N_2-flow (heating rate 5 K/min) and the resulting catalyst was denoted as Pt/CNF-973.

Tin and gallium were deposited on Pt/CNF via RDP (see Table 1 for precursors). Pt/CNF (4.00 g; 3.2 wt%) was stirred for 1 h under hydrogen (1.2 bar) in the required solvent (100 mL; see Table 1 for details). Meanwhile, tin and gallium solutions were prepared in their corresponding solvents (see Table 1). Note that $Sn(HCOO)_2$ solutions were prepared by dissolving SnC_2O_4 in 60 wt% formic acid, which was prepared from concentrated formic acid (Merck). This formic acid solution (60 wt%) was previously adjusted to a pH value of 3.9 using ammonium hydroxide (Merck, conc.), as was described by Meima et al. [20]. Next, 5 mL of the promoter solutions were added via a septum to the Pt/CNF slurry and the mixture was stirred for another 30 min under hydrogen atmosphere. The slurry was filtered and the catalysts were successively dried overnight at 393 K, reduced and heat-treated as described for Pt/CNF-973. The intended Pt/Sn molar ratios on the catalysts were 5, 3, and 1 when $SnCl_4$ was used and thus prepared catalysts were denoted respectively as: Pt–SnCl4/RDP-5, Pt–SnCl4/RDP-3 and Pt–SnCl4/RDP-1. When $Sn(HCOO)_2$ and $Ga(NO_3)_3$ were used, the intended Pt/promoter molar ratio was 5. These catalysts were denoted as Pt–SnForm/RDP-5 and Pt–Ga/RDP.

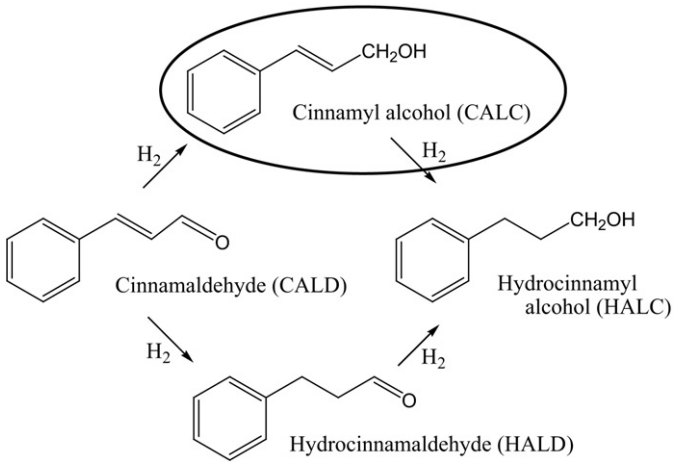

Fig. 1. The hydrogenation pathway of cinnamaldehyde; the desired product is encircled.

For reasons of comparison, tin was also added via incipient wetness impregnation (IWI). Pt/CNF-973 (2.2 g; 3.0 wt%) was evacuated for 30 min. Subsequently, $SnCl_4{\cdot}5H_2O$ (Sigma–Aldrich) was dissolved in demineralized water and 0.85 g of the tin-solution was impregnated on the catalyst, resulting in a platinum/tin molar ratio of 5. The impregnated catalyst was kept under static vacuum for 40 h, dried overnight at 393 K at ambient conditions and reduced as described for Pt/CNF. The resulting catalyst was denoted as Pt–SnCl4/IWI-5.

The catalysts were tested for the cinnamaldehyde hydrogenation at low (1.2 bar) and at high (30 bar) hydrogenation pressure. The hydrogenation of cinnamaldehyde (CALD) can result in cinnamyl alcohol (CALC), hydrocinnamaldehyde (HALD) and the fully hydrogenated product hydrocinnamyl alcohol (HALC) (Fig. 1). The formation of CALC is desired [5,18]. Low pressure tests were performed at 313 K and 1.2 bar H_2 as described earlier [4]. The solvent used was 2-propanol/water and 1 g of catalyst (sieve fraction 25–90 μm) per run was used.

High pressure tests were performed at 313 K and 30 bar H_2 in a batch wise mode. The stainless steel autoclave reactor (Autoclave Engineers, USA) was equipped with gas inlet, stirrer and temperature and pressure control. The catalyst (0.2 g; sieve fraction 25–90 μm) was suspended in a mixture of isopropanol (189.2 mL; Merck, p.a.), demineralized water (30.8 mL) and *t*-cinnamaldehyde (0.33 g; Sigma-Aldrich; p.a.). The slurry was heated to 313 K and saturated with hydrogen without stirring. Next, the reaction was started by starting to stir (1500 rpm) and samples were taken at different time intervals for 90 min. Samples were analyzed using GC Agilent 6890N equipped with autoinjector, FID detector and Agilent DB-1 column. Initial cinnamaldehyde hydrogenation activities were calculated for all tests. The conversion of CALD and selectivity to CALC were calculated as described before [4].

Platinum weight-loadings were determined either using calibrated X-ray fluorescence or ICP-OES. X-ray fluorescence analysis was performed on a calibrated Spectro X-lab 2000 apparatus using 2–4 g of the dry catalyst powder. ICP-OES, which was also used to analyze the gallium loading, was performed on a SPECTRO CIROS^{CCD} ICP-Spectrometer. Each sample was destructed by heating in aqua regia (1:3 mixture of HNO_3:HCl) before analysis. For Pt–SnCl4/RDP-1, the tin loading was determined by analyzing the amount of tin left in the filtrate solution using ICP-OES on the same apparatus as described above.

TEM was performed on a Tecnai 20 FEG operating at 200 kV (point resolution of 2.7 Å). The instrument was equipped with an EDAX EDS system, a STEM option and a Gatan Imaging Filter 2000. Samples were suspended in ethanol using an ultrasonic treatment and brought onto a holey carbon film on a copper grid.

Hydrogen chemisorption measurements were performed using a Micromeritics ASAP 2020. Samples were dried at 373 K in vacuum followed by cooling to room temperature. Next, the samples were re-reduced in flowing hydrogen at 473 K for 60 min (heating rate 5 K/min). Afterwards, the samples were degassed for at least 30 min at a pressure of <13.3 Pa at 473 K to remove chemisorbed hydrogen and water. The isotherms were measured at 313 K and the mass was determined afterwards. The presented H/Pt ratios are based on the amounts of hydrogen adsorbed at zero pressure, which are calculated by extrapolation of the linear part of the isotherm and the amount of platinum in the sample. Nitrogen physisorption measurements were performed as described earlier [4].

The XPS data were obtained with a Vacuum Generators XPS system, using a CLAM-2 hemispherical analyzer for electron detection. Non-monochromatic Al ($K\alpha$) X-ray radiation was used for exciting the photoelectron spectra using an anode current of 20 mA at 10 keV. The pass energy of the analyzer was set at 50 eV.

Sn K and Pt L_3 XAFS spectra for several catalysts were either measured at HasyLab (beamline C) in Hamburg equipped with a Si(311) double-crystalmonochromator (detuned to 70% of maximum intensity to avoid higher harmonics present in the X-ray beam) or at the ESRF (beamline BM26A DUBBLE) in Grenoble equipped with a Si(111) double-crystalmonochromator (higher harmonics were reduced by the presence of a secondary Si mirror after the crystalmonochromator). Pt L_3 spectra were measured in transmission mode and Sn K spectra were measured in the fluorescence mode. For the latter measurements, self-absorption of the fluorescence signal was negligible due to the low tin-loading on the samples. The powdered catalysts were pressed into self-supporting wafers and mounted in a stainless-steel in situ cell equipped with Kapton windows, resulting in a total absorption of 0.5–0.7 for the Pt L_3 transmission measurements. The samples were re-reduced in situ at 473 K for 60 min (5 K/min) in flowing hydrogen, cooled down in hydrogen atmosphere and XAFS data were collected ($T = 77$ K). Three scans were averaged and the EXAFS data from the measured absorption spectra were extracted with the XDAP code (version 2.2.7, 2006) [21]. Preedge subtraction, background subtraction and normalization of the data were performed as described by Toebes et al. [1]. The phase shift and backscattering amplitude functions for the Pt–Sn absorber–backscatterer pair at the Pt L_3 edge, was extracted from experimental XAFS data using a Pt–Sn complex, i.e. $(Pt(SnCl_3)_5)\cdot(Ph_3PCH_3)_3$ ($N = 5$, $R = 2.57$ Å, k-range = 2.3–14.3 Å^{-1}, k^1-weighting, filtered FT range = 1.7–2.9 Å [22]). This complex was prepared as described by Nelson et al. (according to method A) [23]. The reference data for Pt–Sn was measured at the same temperature as the samples ($T = 77$ K) and the first shell scattering atoms (Pt–Sn) were well separated from the higher shells. Therefore, back transformation of the first shell in the Fourier-transformed data was used to obtain the backscattering amplitude and phase shift function of the Pt–Sn absorber–backscatterer pair. Phase shift and backscattering amplitude functions for Pt–Pt and Pt–O were obtained from FEFF7 as described by Van Dorssen et al. [24]. For Sn–Pt, Sn–Cl, Sn–O and Sn–Sn absorber–backscatterer pairs (see also [22]) these functions were obtained from FEFF8. In Table 2 the used parameters for the FEFF8 calculations are summarized. Backscattering amplitude and phase shift functions were optimized with respect to S_0^2 and V_r. These functions were accepted when they could successfully describe the first shells of experimentally measured tin(II)oxide for Sn–O and Sn–Sn (i.e. Sn^{2+}–Sn^{2+}) absorber–backscatterer pairs, and for experimentally measured $(Pt(SnCl_3)_5)\cdot(Ph_3PCH_3)_3$ for Sn–Pt and Sn–Cl absorber–backscatterer pairs with respect to the expected values for distance and coordination number [22,25]. Data analysis of the catalysts was performed by multiple shell fitting using the difference file technique in R-space ($1.0 < R < 3.5$ Å) with the XDAP code using both k^1 and k^3 weighting [26]. Variances of the fits were calculated as described earlier [1].

Table 2
Used input parameter for FEFF8 calculations.[a]

Absorber–backscatterer	N	R (Å)	S_0^2	σ^2 (Å^{-1})	V_r (eV)	V_i (eV)	Reference compound
Sn–Pt	1	2.57	1	0	0	1	Pt–Sn complex
Sn–Cl	1	2.28	1	0	0	1	Pt–Sn complex
Sn–O	1	2.22	1	0	12	1	Tin(II)oxide
Sn–Sn	1	3.54	0.9	0	5	1	Tin(II)oxide

[a] Hedin–Lundqvist potentials were used for calculations.

Table 3
Physical and chemical properties of the catalysts.

Sample	Intended promoter loading (wt%)	Actual promoter loading (wt%)	H/Pt ratio based on H_2-chemisorption	Average particle size based on TEM (nm)	XPS Sn $3d_{5/2}$ peak maximum (eV)
Pt/CNF-973			0.45	2.0	–
Pt–SnCl4/RDP-5	0.4	n.a.	0.32	2.3	486.0
Pt–SnCl4/RDP-3	0.6	n.a.	0.17	2.8	486.0
Pt–SnCl4/RDP-1	1.8	0.7	0.22	3.2	486.0
Pt–SnForm/RDP-5	0.4	n.a.	0.32	n.a.	486.0
Pt–SnCl4/IWI-5	0.4	0.4	0.41	2.0	486.8
Pt–Ga/RDP	0.2	0.1	0.33	2.1	–

n.a. = not analyzed.

3. Results and discussion

All samples had a BET surface area of about 180 m^2/g and a mesopore volume of about 0.26 mL/g. No micropores were found. The platinum loading was similar for all samples (3.0 to 3.3 wt%). In Table 3 the intended and for some catalysts also the actual promoter loadings are summarized. The gallium loading in Pt–Ga/RDP was 0.1 wt%. The actual tin weight loading for Pt–SnCl4/RDP-1 (0.7 wt%) was lower than the intended loading (1.8 wt%) thus it must be concluded that high loadings were not achieved by RDP. This can be expected since the theoretical maximum weight-loading is about 0.8 wt% when assuming a $Sn/Pt_{surface}$ of 1 and a H/Pt ratio of 0.45 (Table 3). Nevertheless we intended for a higher loading to obtain the highest possible actual tin loading.

The number of accessible available platinum sites was determined using hydrogen chemisorption. The hydrogen chemisorption results are also summarized in Table 3 and expressed as H/Pt ratio. The highest H/Pt ratio was observed for monometallic Pt/CNF-973. In general an increasing intended tin-loading resulted in a lower H/Pt ratio for the RDP prepared samples. This suggests that upon deposition of higher concentrations of promoter, a lower amount of hydrogenation sites is available on the catalysts, which can be ascribed to an increased coverage of platinum by tin. This indicates that tin is well dispersed over the platinum surface which suggests a good contact between platinum and tin for RDP prepared samples. For the sample prepared by IWI the decrease in hydrogen chemisorption capacity was less significant. Thus indicating that tin was not, to a significant extent, present on the platinum surface, i.e. not in close contact.

TEM-EDX was used to determine platinum particle sizes (Table 3), size distributions and chemical composition of the samples. In Fig. 2 representative TEM images are displayed for Pt–SnCl4/IWI-5, Pt–SnCl4/RDP-5, Pt–SnCl4/RDP-3 and Pt–SnCl4/RDP-1. In

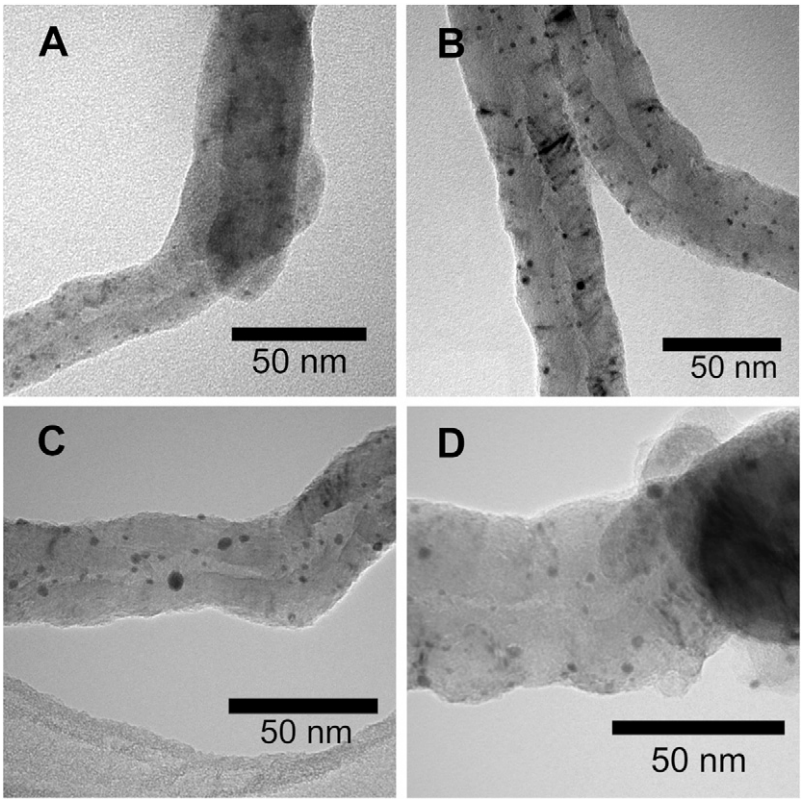

Fig. 2. TEM images of (A) Pt–SnCl4/IWI-5 (1–3 nm), (B) Pt–SnCl4/RDP-5 (1–4 nm), (C) Pt–SnCl4/RDP-3 (1–6 nm), (D) Pt–SnCl4/RDP-1 (1–7 nm).

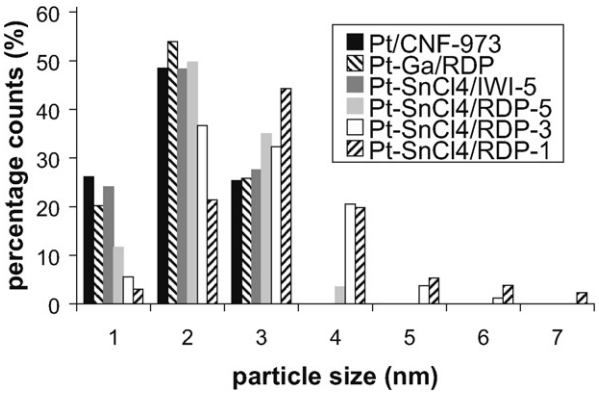

Fig. 3. TEM histograms of the analyzed samples showing the particle size distribution for several catalysts.

Fig. 3 the platinum particle size distributions for the latter samples and for Pt–Ga/RDP and Pt/CNF-973 are shown. For Pt/CNF-973, Pt–Ga/RDP and Pt–SnCl4/IWI-5 a platinum particle size range of 1–3 nm is observed. After deposition of tin via RDP, the platinum particle size range increased i.e., 1–4 nm for Pt–SnCl4/RDP-5, 1–6 nm for Pt–SnCl4/RDP-3 and 1–7 nm for Pt–SnCl4/RDP-1. Increasing metal particle sizes upon addition of larger amounts of tin has been observed as well by Neri et al. [27]. Apparently, combining monometallic platinum catalysts with tin via RDP resulted in larger platinum particles, i.e. sintering, after reduction.

Dark field TEM images and elemental maps obtained via EDX analysis are shown in Fig. 4 for Pt–SnCl4/RDP-3 and for Pt–Ga/RDP. Analysis of the elemental maps was limited to areas of 25 nm. For both samples it was observed that the presence of platinum and tin or platinum and gallium, which are depicted as the brighter areas in Fig. 4, coincide at this scale. Based on this characterization technique, it is therefore tentatively concluded that platinum and promoters are in close vicinity.

To get a more detailed picture of the interaction between platinum and tin, XAFS studies both on the Pt L_3 and Sn K edge for Pt–SnCl4/RDP-5, Pt–SnCl4/RDP-1 and Pt–SnCl4/IWI-5 were performed. The absorption edge energy position measured for the Pt L_3 spectra was at 11564 eV, corresponding to platinum in the metallic state. Results of the data fitting are reported in Table 4A. For the raw, Fourier-transformed and fitted data we refer to supplementary information. The number of free parameters (N_I) which are allowed to use for the fitting procedure, is calculated using $N_I = (2\Delta k \Delta R/\pi) + 2$ (Δk: Fourier transform range of the raw data, ΔR: fit range) [28]. For the Pt L_3-fits it is calculated that $N_I = 14.9$. Since the Pt–Pt distance is known (i.e. 2.76–2.77 Å [24,29]), this parameter was fixed for all fits thereby allowing 4 shells for fitting. The low variances of the fit indicate that the data could be fitted well with the given parameters. For all samples Pt–Pt, Pt–Sn and two Pt–O (long: PtOl and short: Pt–Os) contributions were found. The latter is in agreement with observations of Zhang et al. [29] for reduced platinum on CNF catalysts. Platinum EXAFS is mainly dominated by the Pt–Pt contributions and its coordination number increased from 5.7 to 6.7 when going from Pt–SnCl4/IWI-5, Pt–SnCl4/RDP-5 to Pt–SnCl4/RDP-1. This indicates that the platinum particles sizes increased with increasing tin content which is in agreement with the above discussed TEM results.

When assuming spherical particles, the resulting Pt–Pt coordination numbers (5.7 to 6.7) correspond to particle sizes of 1.1–1.4 nm in diameter [30]. Table 3 indicated that the particle sizes determined by TEM are around 2 nm. This discrepancy in particle size has been observed earlier for small particles and has been ascribed to the fact that TEM may not detect the metal particles smaller than about 1 nm thereby resulting in overestimation of the average particle size [29]. EXAFS on the other hand averages over all platinum coordination numbers thus including also the very small particles which results in a lower average particle size.

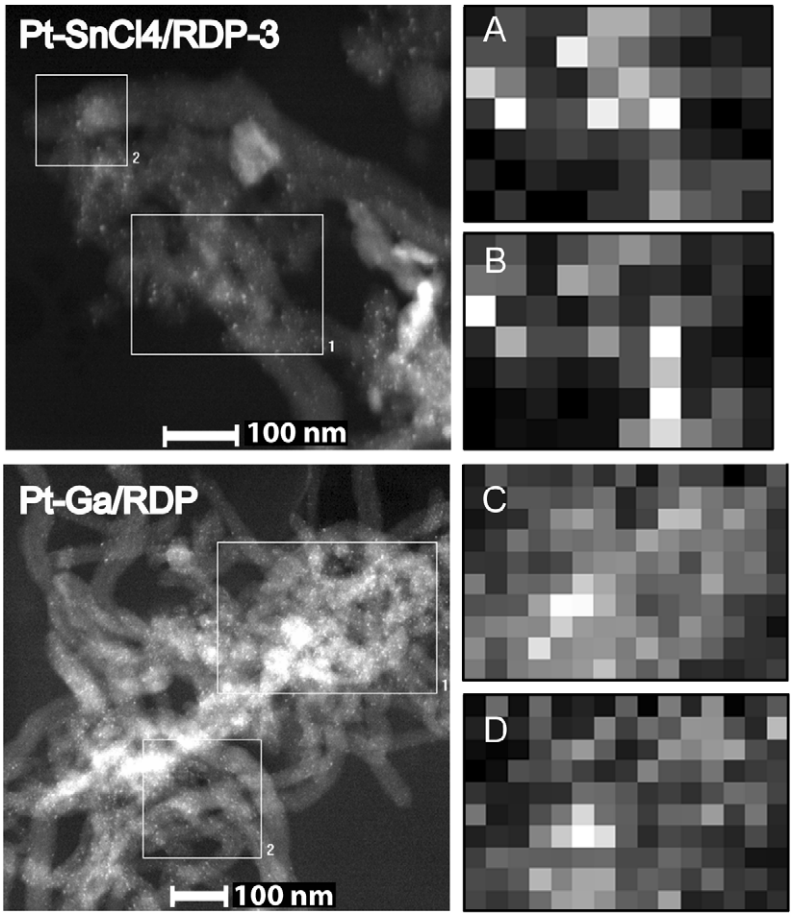

Fig. 4. TEM dark field images of Pt–SnCl4/RDP-3 and Pt–Ga/RDP. Elemental EDX maps were taken from area 1. Area 2 was used to correct for any drift of the samples. Map (A) reflects the measured Sn L intensity and map (B) the measured Pt M intensity of Pt–SnCl4/RDP-3. Map (C) reflects the measured Ga L intensity and map (D) the measured Pt M intensity of Pt–Ga/RDP. Going from dark to light correspond to increasing metal intensities.

Table 4
EXAFS fit results for the analyzed catalysts at the Pt L_3-edge or Sn K-edge using four or three different absorber–backscatterer pairs (scatter). The resulting coordination numbers (N), scatter distances (R), Debye–Waller factor ($\Delta\sigma^2$) and energy shifts are summarized. The k-range, R-space and variances of the magnitude and imaginary part of the Fourier-transforms are also summarized.

Catalyst	Scatter	N	R (Å)	$\Delta\sigma^2$ (Å^2) $\times10^{-3}$	ΔE_0 (eV)	Δk (Å^{-1})	ΔR (Å)	k^1 variance (%)	
								Abs	Im
(A) Fit results at Pt L_3-edge									
Pt–SnCl4/IWI-5	Pt–Pt	5.7	2.76	2.7	0.9	3.0–14.3	1.5–3.3	0.34	0.95
	Pt–Os	1.0	1.99	9.7	2.9				
	Pt–Ol	0.7	2.61	2.3	3.5				
	Pt–Sn	0.5	2.74	4.2	3.0				
Pt–SnCl4/RDP-5	Pt–Pt	6.4	2.76	1.7	2.5	3.0–14.3	1.5–3.3	0.18	0.36
	Pt–Os	0.4	2.00	9.0	4.2				
	Pt–Ol	0.8	2.62	3.8	0.9				
	Pt–Sn	0.8	2.75	6.2	0.1				
Pt–SnCl4/RDP-1	Pt–Pt	6.7	2.76	3.0	4.0	3.0–14.3	1.5–3.3	0.15	0.81
	Pt–Os	0.6	2.00	9.9	1.2				
	Pt–Ol	0.4	2.63	4.1	2.4				
	Pt–Sn	1.2	2.73	6.4	4.5				
(B) Fit results at Sn K-edge									
Pt–SnCl4/IWI-5	Sn–Sn	0.5	3.18	2.1	2.2	3.5–12.4	1.0–3.3	0.28	0.77
	Sn–Pt	1.6	2.71	7.8	−6.9				
	Sn–O	5.1	2.04	9.4	5.4				
Pt–SnCl4/RDP-5	Sn–Sn	–	–	–	–	2.9–12.0	1.2–3.5	0.35	0.60
	Sn–Pt	4.8	2.74	9.9	−6.1				
	Sn–O	1.1	2.08	9.9	5.9				
Pt–SnCl4/RDP-1	Sn–Sn	0.6	3.34	7.2	−6.9	2.85–12.0	1.2–3.5	0.45	0.82
	Sn–Pt	5.2	2.75	8.0	−5.7				
	Sn–O	0.8	2.06	9.9	6.9				

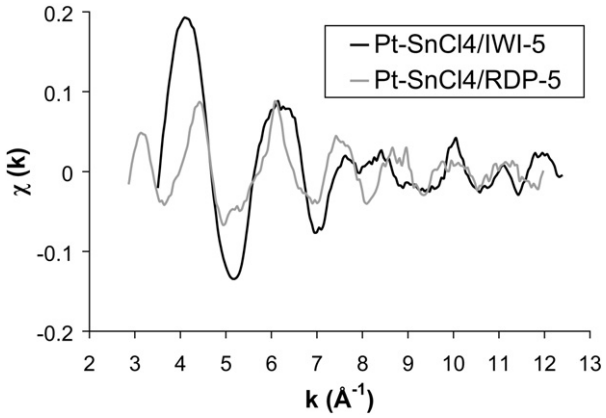

Fig. 5. The experimental Sn K EXAFS data (k^1 weighted) of Pt–SnCl4/IWI-5 ($\Delta k = 3.5$–12.4 Å^{-1}) and Pt–SnCl4/RDP-5 ($\Delta k = 2.9$–12.0 Å^{-1}).

The coordination numbers for the Pt–O contributions at long and at short distance do not show a trend as function of the synthesis method. Moreover, the coordination numbers are small, i.e. 0.4–1.0, and therefore, definite conclusions with respect to these contributions were not drawn.

The Pt–Sn contribution was the lowest (0.5) for Pt–SnCl4/IWI-5 and increased to 0.8 and 1.2 for Pt–SnCl4/RDP-5 and Pt–SnCl4/RDP-1. These coordination numbers are also rather small, though it indicates that RDP resulted in more tin atoms being in close contact with platinum as compared to IWI, which is in agreement with the hydrogen chemisorption results described above. Moreover, a higher tin-loading for RDP prepared samples also resulted in a higher concentration of tin in close contact with platinum. This is also in agreement with the hydrogen chemisorption results.

Platinum–tin interactions were also investigated using Sn K-edge XAFS. The absorption edge energy position for the RDP prepared samples (29201.2 eV) was close to the absorption edge energy of tin(II)oxide reference material (29201.7 eV) indicating the presence of tin(II). Thus tin became reduced during RDP synthesis and the subsequent reductive treatment, since originally tin(IV) was used at the start of the synthesis. For the IWI synthesized sample, a stronger white line, as compared to the RPD samples, is observed and its edge position shifted by about 2 eV to higher energy which is close to the edge position of tin(IV)oxide reference material (i.e., 29203.5 eV). Hence, tin does not become reduced when deposited via IWI. The reduction of tin for RDP-prepared samples is speculated to result from the interaction of tin obtained with the hydrogen saturated platinum surface.

In Fig. 5 the background subtracted and normalized Sn K-edge EXAFS data of Pt–SnCl4/IWI-5 and Pt–SnCl4/RDP-5 are depicted as representative examples and indicate a good signal/noise ratio up to $k = 12$. The resulting EXAFS data were fitted and fit results are compiled in Table 4B. The number of free parameters for the Sn K-edge fits ranges from 15.0–15.4, which allows the use of 3 shells for fitting. Figs. 6 and 7 show the Fourier-transformed plots of the experimental and fitted data for Pt–SnCl4/IWI-5 and Pt–SnCl4/RDP-5.

The fit results for Pt–SnCl4/IWI-5 show that a substantial Sn–O contribution is observed with a coordination number of 5.1, while the Sn–Pt and Sn–Sn contributions are 1.6 and 0.5, respectively. The Sn–O (2.04 Å) and Sn–Sn (3.18 Å) distances found here correspond to that of tin(IV)oxide [31]. Moreover, a strong white line is observed, indicating tin is in a high oxidation state and in addition, the edge position is close to tin(IV)oxide. This shows that small tin(IV)oxide clusters were present which were not in close contact with platinum.

This is in contrast to the RDP prepared catalysts which resulted in significant Sn–Pt contributions with coordination numbers of

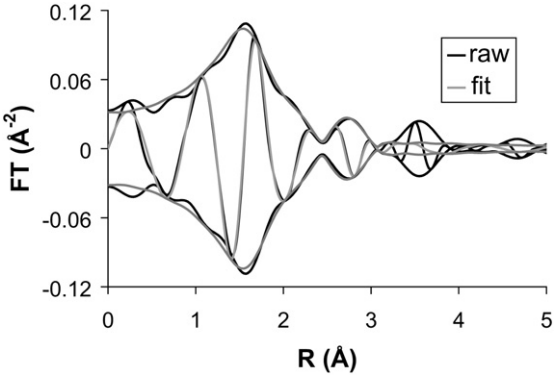

Fig. 6. The Sn K Fourier-transform of the data and the fit for Pt–SnCl4/IWI-5 (k^1 weighted; $\Delta k = 3.5$–12.4 Å^{-1}; $\Delta R = 1.0$–3.3 Å).

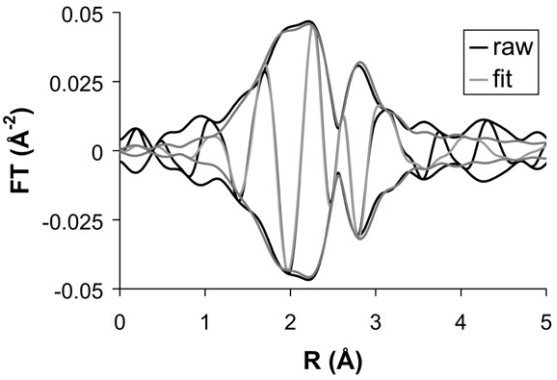

Fig. 7. The Sn K Fourier-transform of the data and the fit for Pt–SnCl4/RDP-5 (k^1 weighted; $\Delta k = 2.9$–12.0 Å^{-1}; $\Delta R = 1.2$–3.5 Å).

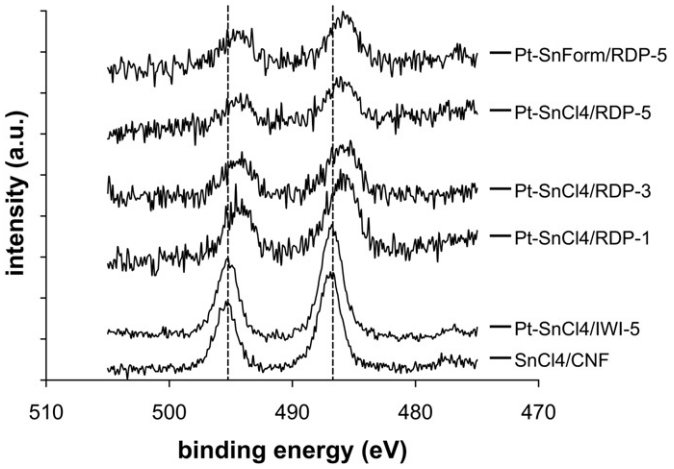

Fig. 8. The measured XPS Sn $3d_{3/2}$ (left peak) and Sn $3d_{5/2}$ (right peak) of the bimetallic samples. The vertical dotted lines indicate the peak maxima for the reference material, which was prepared via impregnation and treatment at 473 K in H_2/N_2 of $SnCl_4$ on CNF.

4.8 and 5.2 for Pt–SnCl4/RDP-5 and Pt–SnCl4/RDP-1, respectively. These results show that RDP leads to a close contact of tin on platinum, thereby forming a bimetallic system, while for the IWI sample this interaction is low. The coordination numbers for Sn–O for Pt–SnCl4/RDP-5 and Pt–SnCl4/RDP-1 are low (1.1 and 0.8, respectively) and therefore, firm conclusions with respect to this contribution cannot be drawn. The Sn–Sn contribution is low (coordination number of 0.6) for Pt–SnCl4/RDP-1 and could not be determined at all for Pt–SnCl4/RDP-5, which is again an indication that large tin oxide clusters were not formed by RDP. The distance

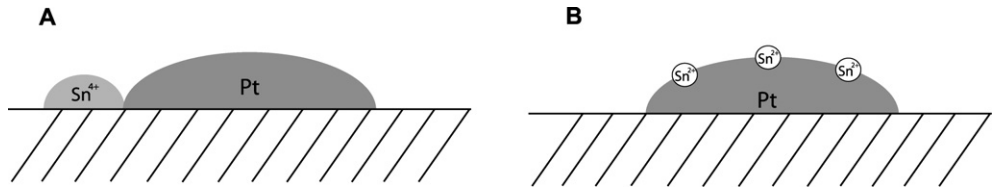

Fig. 9. Schematic representation of the location of the tin cations in (A) platinum–tin catalyst prepared via IWI and (B) platinum–tin catalyst prepared via RDP.

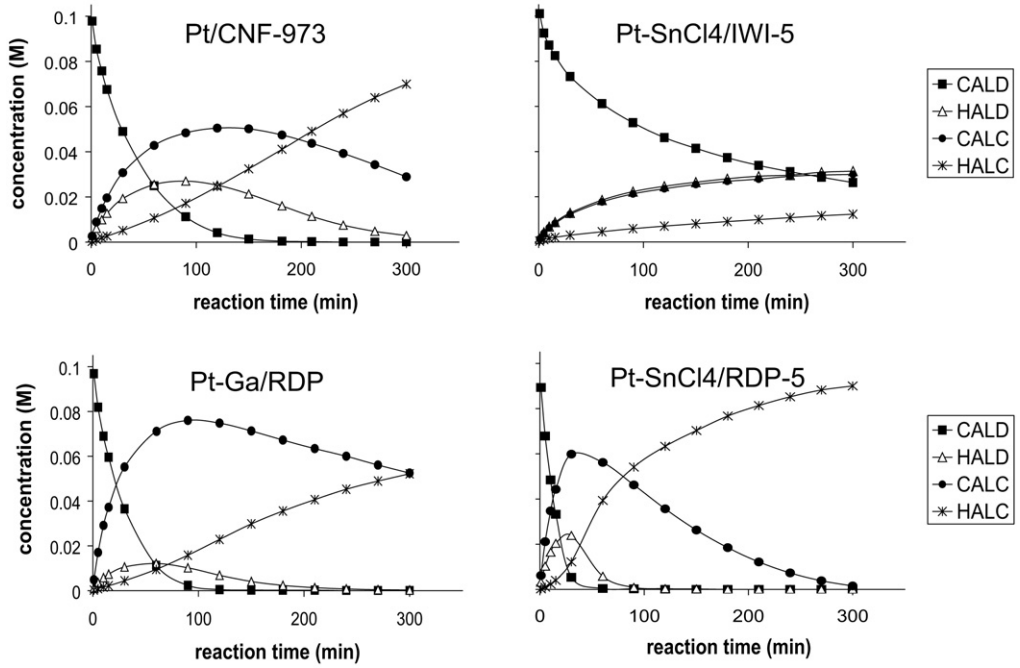

Fig. 10. Cinnamaldehyde hydrogenation results of several of the tested catalysts. Test reactions were performed at 313 K under 1.2 bar H_2 in 2-propanol/water mixture.

for the Sn–O contribution (i.e., 2.06–2.08 Å) is lower than expected for tin(II)oxide (i.e., 2.2 Å [25]), which indicates that this oxygen has a different nature as compared to that in tin(II)oxide.

All platinum–tin catalysts were analyzed using XPS for platinum, tin, carbon, and oxygen. Chlorine, if present, was below the detection limit for all analyzed samples. The measured Sn 3d peak position is depicted in Fig. 8 and the Sn $3d_{5/2}$ peak maximum positions are summarized in Table 3. For reasons of comparison, a reference material was prepared by impregnation and treatment of $SnCl_4$ on CNF at 473 K in H_2/N_2 flow, referred to as SnCl4/CNF. Synthesis of platinum–tin on CNF via IWI did not result in a shift of the peak maxima when compared to the reference sample, while synthesis via RDP resulted in a shift of the peak maxima to lower binding energies close to tin(II) reference species [32]. Such a peak shift has not been observed for any of the other measured elements, i.e. platinum, carbon and oxygen. Both XAFS analysis as well as XPS analysis techniques indicated the presence of tin(II) for RDP-synthesized catalysts and tin(IV) for the IWI-synthesized catalyst. Please, note that XAFS measurements were measured in situ directly after reduction, while the XPS samples were shortly exposed to air before the measurements. Since the results agree with each other, it is concluded that tin is not reoxidized due to air exposure. The observed tin reduction is only possible when close interaction of tin with the hydrogen saturated platinum surface is present.

Thus to summarize, using TEM-EDX, EXAFS and XPS it is demonstrated that RDP resulted in a close contact of the two metals and partial reduction of tin on the platinum sites, which is not observed for the IWI prepared catalyst. A schematic representation of these catalysts is depicted in Fig. 9.

The catalysts were tested for CALD hydrogenation at low pressure and for some catalysts also at high pressure. Representative examples of the low-pressure test reactions are displayed in Fig. 10. In Table 5 the initial hydrogenation activities, the reaction time required to obtain 50% CALD conversion and the selectivity towards CALC are shown. From Fig. 10 and Table 5 it can be seen that at low pressure, catalysts prepared via RDP are more selective and active compared to the monometallic catalyst. The platinum–gallium catalyst resulted in the highest selectivity at this pressure. In contrast to the RDP prepared catalysts, the IWI prepared catalyst resulted in a decreased activity and selectivity as compared to the monometallic Pt/CNF. It has been observed that for all test reactions (also when performed at high pressure) <3.8% by-products were formed. These by-products were mainly propylbenzene and β-methylstyrene, while ethylbenzene has not been observed for any test reaction. Only for Pt–SnCl4/IWI-5 the formation of acetals, 0.5%, was observed during testing. For this catalyst tin(IV) species are present as promoter and we believe that this is mainly in the form of tin(IV)oxide, since chlorine has not been detected using XPS. It has been described earlier that the presence of tin(IV)oxide may result in the formation of acid sites on the catalyst surface, which is associated with acetal formation [33,34]. The formation of this type of by-products often result in a decreasing catalytic activity and selectivity [33,34].

Industrial application of CALD hydrogenations are in general performed at high hydrogenation pressures [35]. Therefore some catalysts were tested at high hydrogenation pressures (30 bar) to investigate catalytic behavior under these conditions. In Table 5 an overview of the obtained test results is given for the following catalysts: Pt–SnCl4/RDP-5, Pt–SnForm/RDP-5, Pt–SnCl4/IWI-5,

Table 5
Results of the catalytic tests.

Sample	Low pressure tests			High pressure tests		
	Initial activity ($mmol\,s^{-1}\,g_{Pt}^{-1}$)[a]	Reaction time (min)[b]	Selectivity (%)[c]	Initial activity ($mmol\,s^{-1}\,g_{Pt}^{-1}$)[a]	Reaction time (min)[d]	Selectivity (%)[e]
Pt–SnCl4/RDP-5	0.37	10	72	0.59	4.5	42
Pt–SnCl4/RDP-3	0.32	12	79	n.t.	n.t.	n.t.
Pt–SnCl4/RDP-1	0.27	15	81	n.t.	n.t.	n.t.
Pt–SnForm/RDP-5	0.29	13	74	0.49	5.0	31
Pt–SnCl4/IWI-5	0.18	85	43	0.55	5.5	17
Pt–Ga/RDP	0.25	20	88	0.40	8.0	39
Pt/CNF-973	0.21	30	59	0.75	3.5	19

n.t. = not tested.
[a] Initial activity based on the first two reaction data points.
[b] Reaction time (min) required to reach 50% CALD conversion at low pressure.
[c] Selectivity to CALC (%) at 50% CALD conversion at low pressure.
[d] Reaction time (min) required to reach 50% CALD conversion at high pressure.
[e] Selectivity to CALC (%) at 50% CALD conversion at high pressure.

Pt–Ga/RDP and Pt/CNF-973. Please note that some screening experiments, in which either the catalyst particle sizes or stirring speeds were varied, indicated that the selectivity was not affected by the presence or absence of mass transfer limitation. As for the low pressure experiments also at high hydrogenation pressure, RDP synthesized bimetallic catalysts resulted in enhanced selectivities irrespective the used precursor, while the IWI prepared catalyst resulted in a slightly lower selectivity compared to the monometallic catalyst. This means that the observed trend with respect to selectivity both at low and at high hydrogenation pressure is the same. It must be noted here that Pt–SnCl4/RDP-5 resulted in a higher selectivity compared to Pt–Ga/RDP, which is not expected based on the low hydrogenation pressure results. An explanation for the latter behavior is lacking.

To investigate the stability of the catalyst we filtered the reaction mixture after a catalytic run. The solvent in the filtrate was evaporated and the resulting solid was treated in aqua regia and analyzed for leached platinum using ICP-OES. Since no platinum was detected it was concluded that leaching did not occur.

The absolute selectivities decreased when comparing high pressure test reactions with low pressure test results. In literature, it has been reported that higher CALD concentrations resulted in a higher selectivity [36,37]. It has also been reported that higher hydrogenation pressures can result in a lower selectivity compared to lower hydrogen pressures [34,37]. Since in this study the hydrogenation pressure was increased and the CALD concentration was decreased at the same time when going from the low to the high pressure experiments, a combination of these two factors might have resulted in the observed decrease in absolute selectivities at high pressure.

At higher pressure the activity of Pt/CNF was higher compared to that of the bimetallic catalysts, while the opposite trend is observed for the low pressure tests. It has been reported before that the addition of a second metal can result an increasing as well as a decreasing activity [5,34,38]. Increased activities have been ascribed to the presence of ionic promoters directing the C=O bond towards the platinum, thereby enhancing both selectivity and activity. Decreased activities have been ascribed to the presence of high promoter concentrations resulting in a dramatically decreasing hydrogenation capacity [5]. Our results suggest that the optimum activity does not depend on a particular amount of promoter only, but may shift due to application of different test conditions as well. Since multiple variables are present when comparing high pressure tests to low pressure tests, e.g. different reactant concentrations and different hydrogenation pressures, this behavior cannot be ascribed to one particular reaction parameter yet.

For RDP synthesis we reported that platinum does sinter after reduction and heat-treatment (Table 3). In our previous study, it is concluded that for heat-treated platinum on CNF larger metal particles result in a decreasing selectivity [4]. Therefore, the selectivity increase observed here can only be attributed to the presence of promoters and not to the presence of larger platinum particles.

The RDP synthesis results in close contact of tin with platinum, thereby forming a close interaction of the two metals. This results in a higher selectivity to cinnamyl alcohol for the cinnamaldehyde hydrogenation, irrespective the applied hydrogenation pressure. The increase in selectivity observed with RDP synthesized catalysts is not observed for the bimetallic catalyst prepared via IWI synthesis where close platinum–tin interaction is absent.

4. Conclusions

In this study, tin and gallium promoted Pt/CNF catalysts were prepared by reductive deposition precipitation (RDP, i.e. deposition under hydrogen atmosphere) and incipient wetness impregnation (IWI). TEM-EDX, XPS and EXAFS showed that RDP synthesis resulted in a close contact between promoter and platinum. Catalysts which displayed a close and significant contact between platinum and promoter were more selective in the hydrogenation of cinnamaldehyde to cinnamyl alcohol as compared to the samples in which such an interaction is not present. For activity such a clear conclusion could not be drawn since activity is mainly influenced by the reaction conditions, such as pressure and reactant concentration.

Acknowledgments

The authors wish to acknowledge the following people: Ad Mens (XPS and nitrogen physisorption), Prof. Ir. John Geus (TEM-EDX), Cor van der Spek (TEM) and Helen de Waard (ICP-OES). Also Korneel Cats, Maarten van Heek, Robin Jastrzebski and Jeroen Pet are acknowledged for their contribution to this work. The synchrotron stations C at HASYLAB (Hamburg, Germany, EU project no. I-20060150EC) and BM26A at ESRF (Grenoble, France, NWO project no. 26-01-767) are acknowledged for the allocated beamtime. Financial support was provided by EU Nanocat Project 506621.

Supplementary information

The online version of this article contains additional supplementary information.

Please visit DOI: 10.1016/j.jcat.2009.02.003.

References

[1] M.L. Toebes, Y. Zhang, J. Hájek, T.A. Nijhuis, J.H. Bitter, A.J. van Dillen, D.Y. Murzin, D.C. Koningsberger, K.P. de Jong, J. Catal. 226 (2004) 215.
[2] M.L. Toebes, T.A. Nijhuis, J. Hájek, J.H. Bitter, A.J. van Dillen, D.Y. Murzin, K.P. de Jong, Chem. Eng. Sci. 60 (2005) 5682.
[3] M.L. Toebes, M.K. van der Lee, L.M. Tang, M.H. Huis in't Veld, J.H. Bitter, A.J. van Dillen, K.P. de Jong, J. Phys. Chem. B 108 (2004) 11611.
[4] A.J. Plomp, H. Vuori, A.O.I. Krause, K.P. de Jong, J.H. Bitter, Appl. Catal. A 351 (2008) 9.
[5] P. Gallezot, D. Richard, Catal. Rev. Sci. Eng. 40 (1998) 81.
[6] V. Ponec, Appl. Catal. A 149 (1997) 27.
[7] W.F. Tuley, R. Adams, J. Am. Chem. Soc. 47 (1925) 3061.
[8] D. Richard, J. Ockelford, A. Giroir-Fendler, P. Gallezot, Catal. Lett. 3 (1989) 53.
[9] S. Galvagno, A. Donato, G. Neri, R. Pietropaolo, D. Pietropaolo, J. Mol. Catal. 49 (1989) 223.
[10] O.S. Alexeev, B.C. Gates, Ind. Eng. Chem. Res. 42 (2003) 1571.
[11] K.P. de Jong, Curr. Opin. Solid State Mater. Sci. 4 (1999) 55.
[12] J. Barbier, in: G. Ertl, H. Knözinger, J. Weitkamp (Eds.), Preparation of Solid Catalysts, Wiley–VCH, Weinheim, 1999, p. 526.
[13] E. Lamy-Pitara, L. El Ouazzani-Benhima, J. Barbier, J. Electroanal. Chem. 335 (1992) 363.
[14] G. Corro, P. Marecot, J. Barbier, Stud. Surf. Sci. Catal. 111 (1997) 359.
[15] F. Epron, C. Carnevillier, P. Marecot, Appl. Catal. A 295 (2005) 157.
[16] C. Carnevillier, F. Epron, P. Marecot, Appl. Catal. A 275 (2004) 25.
[17] T. Mallat, A. Baiker, Appl. Catal. A 200 (2000) 3.
[18] S. Schimpf, J. Gaube, P. Claus, Springer Ser. Chem. Phys. 75 (2004) 87.
[19] M.L. Toebes, J.H. Bitter, A.J. van Dillen, K.P. de Jong, Catal. Today 76 (2002) 33.
[20] G.R. Meima, B.G. Dekker, A.J. van Dillen, J.W. Geus, J.E. Bongaarts, F.R. van Buren, K. Delcour, J.M. Wigman, Stud. Surf. Sci. Catal. 31 (1987) 83.
[21] M. Vaarkamp, J.C. Linders, D.C. Koningsberger, Physica B 209 (1995) 159.
[22] H.H.C.M. Pinxt, Ph.D. thesis, Eindhoven Univ. Technol., Eindhoven, 1997.
[23] J.H. Nelson, N.W. Alcock, Inorg. Chem. 21 (1982) 1196.
[24] G.E. van Dorssen, D.C. Koningsberger, D.E. Ramaker, J. Phys. Condens. Matter 14 (2002) 13529.
[25] W.J. Moore, L. Pauling, J. Am. Chem. Soc. 63 (1941) 1392.
[26] D.C. Koningsberger, B.L. Mojet, G.E. van Dorssen, D.E. Ramaker, Top. Catal. 10 (2000) 143.
[27] G. Neri, C. Milone, S. Galvagno, A.P.J. Pijpers, J. Schwank, Appl. Catal. A 227 (2002) 105.
[28] E.A. Stern, Phys. Rev. B 48 (1993) 9825.
[29] Y. Zhang, M.L. Toebes, A. van der Eerden, W.E. O'Grady, K.P. de Jong, D.C. Koningsberger, J. Phys. Chem. B 108 (2004) 18509.
[30] A. Jentys, Phys. Chem. Chem. Phys. 1 (1999) 4059.
[31] W.H. Baur, A.A. Khan, Acta Crystallogr. B 27 (1971) 2133.
[32] C.D. Wagner, W.M. Riggs, L.E. Davis, J.F. Moulder, Handbook of X-ray Photoelectron Spectroscopy, Perkin–Elmer Corporation, Eden Prairie, 1979.
[33] M.d.C. Aguirre, P. Reyes, M. Oportus, I. Melian-Cabrera, J.L.G. Fierro, Appl. Catal. A 233 (2002) 183.
[34] P. Maki-Arvela, J. Hajek, T. Salmi, D.Y. Murzin, Appl. Catal. A 292 (2005) 1.
[35] T. Vergunst, Ph.D. thesis, Delft University of Technology, Delft, 1999.
[36] T. Vergunst, F. Kapteijn, J.A. Moulijn, Catal. Today 66 (2001) 381.
[37] M. Shirai, T. Tanaka, M. Arai, J. Mol. Catal. A: Chem. 168 (2001) 99.
[38] G. Neri, S. Galvagno, Recent Res. Devel. Catal. 2 (2003) 121.